Electronic Supplementary Material (ESI) for Physical Chemistry Chemical Physics.

Supporting Information

Electronic conductivity of polymer electrolytes: Electronic charge transport properties of LiTFSI-doped PEO

*Mikael Unge[1,2] *, Harish Gudla[2], Chao Zhang[2], Daniel Brandell[2]**

[1] ABB Corporate Research, SE 72178, Västerås, Sweden

[2] Department of Chemistry - Ångström Laboratory, Uppsala Universitet, SE 75121 Uppsala, Sweden

AUTHOR INFORMATION

Corresponding Author

* Mikael Unge, mikael.unge@se.abb.com, Daniel Brandell, daniel.brandell@kemi.uu.se

COMPUTATIONAL DETAILS – DENSITY FUNCTIONAL THEORY

The electronic structure of the PEO systems are calculated with LS-DFT as implemented in ONETEP via Materials Studio software.[1] The Generalized Gradient Approximation (GGA) functional by Perdew-Burke-Ernzerhof (PBE) and the van der Waals correction by Elstner are used.[2,3] The energy cut-off for the basis is set to 750 eV and the interaction cut-off radius to 17 Å. Conventional DFT calculations is done with CASTEP via Materials Studio software.[4] PBE and PBE0[5] functionals are used in combination with van der Waals correction by Tkatchenko and Scheffler (TS).[6] Energy cut-off values are set to 570 eV and 925 eV for PBE and PBE0, respectively. In order to have an accurate description of conduction band states in the LS-DFT calculations, an optimization of the conduction states can be done.[7] This is particularly needed when the valence and conduction states differ significantly.[7] It has for other electrically insulating polymers been reported that the conduction states are interchain states while the valence states are localize along the polymer backbone.[8,9] It is expected that PEO also follow that the conduction states will be of interchain character and would need to be relaxed to be correctly described.

CRYSTAL PEO – STRUCTURE AND ORBITALS FROM DFT

Calculation of the electronic structure of the crystalline PEO was performed through standard dispersion corrected DFT using both PBE[2] and PBE0[5] with TS[6]. The initial geometry was based on the experimental crystal structure which was followed by a geometry optimization with PBE-TS, see Figure S1. The optimized geometry was also used in single point calculations with the PBE0-TS functional. The lattice parameters of the optimized unit cells is 7.97 Å, 12.78 Å and 19.86 Å with the angle 126.66°, which constitute merely a small deviation from the experimental values.[10]

In literature it has been reported that conduction states of polyethylene (PE) are interchain states.[8] To investigate whether this is the case also for PEO, we used DMol3[11] in Materials Studio and the PBESol functional[12] and TNP[13] basis set to calculate the orbitals of the PEO crystal structure. In Figure S1, the Lowest Unoccupied Molecular Orbital (LUMO) and LUMO+1 are shown. It is clearly seen that these states occupy the free volume in between the chains. The Highest Occupied Molecular Orbital (HOMO) on the other hand, is localized on the polymer chains. Thus, in electronic currents in the crystalline PEO material, the holes will follow the polymer chains while the electrons will jump between free volume pockets.

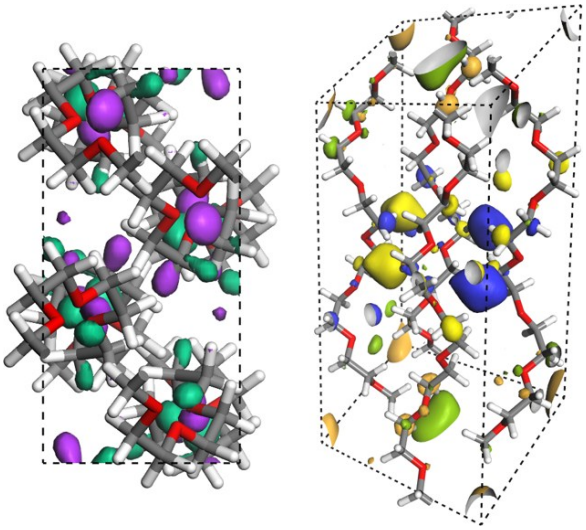

Figure S1 PEO crystal structure with the sides 7.97 Å, 12.78 Å and 19.86 Å with the angle 126.66°. Left: the HOMO is localized to the polymer chains. Right: LUMO (blue-yellow) and LUMO+1 (green-orange) possess a clear interchain character.

MOBILITY EDGE

The electron mobility edge is calculated using a method presented previously.[14,15] Below follow a short review of the methodology in which the orbitals are analyzed using percolation theory. A quantity G_α, grid occupation ratio, for the fraction of grid points of a delocalized state α

occupied by an extra carrier added are analyzed. The quantity G_α is equivalent to the occupation probability in percolation theory. How G_α is calculated is now described. The minimum probability of finding a carrier occupying a delocalized state at a certain grid point belonging to the accessible volume for that state can be written as

$$P_{min} = \frac{1}{\Omega \prod_{i=x,y,z} N_i} \tag{S1}$$

where the N_i's are the number of grid points in respective direction in the simulation cell and Ω is the ratio between the accessible volume and the total volume of the simulation cell. The accessible volume could be the exterior of the van der Waals surface of an amorphous polymer considering the conduction band interchain states of PEO. The probability of finding an electron/hole occupying a state α at a grid point *l* can be written as

$$P_\alpha^l = \frac{C_{l,\alpha}^2}{\sum_k C_{k,\alpha}^2} \tag{S2}$$

where $C_{l,\alpha}$ is the expansion coefficient for the basis function at grid point l describing the electronic state α at that grid point. P_{min} is used as a threshold criterion in the calculations of the quantity G_α, to determine if a specific grid point should be included or not for the state α. If the probability at a grid point is higher than P_{min} indicates that that grid point is important for the description of the localization of that state. If the probability value is lower than P_{min} indicates that the grid point is not important for the description of the state, since the probability is lower than if the state would be completely delocalized. In the method it is thus defined that a grid point l is considered to be important of the wave-function associated with state α, if $P_\alpha^l > P_{min}$. The fraction of grid points which significantly contribute to the state α can be written as

$$G_\alpha(T=0) = \frac{\sum_{P_\alpha^l > P_{min}} 1}{\Omega \prod_{i=x,y,z} N_i} \quad \text{(S3)}$$

To include states accessible within an energy window corresponding to the thermal energy and potential degenerate states we write

$$G_\alpha(T) = \sum_{|E_\alpha - E_\beta| < k_B T} \frac{\sum_{P_\beta^l > P_{min}} 1}{\Omega \prod_{i=x,y,z} N_i} \quad \text{(S4)}$$

where the large sum in front of the fraction is summed over all states β whit an energy difference to the state α, that are smaller than the thermal energy. Hence, from equation (S4) the volume fraction of the orbitals can be determined but in order to determine if the state is delocalized/percolated the shape of the orbitals need to be estimated. This is due to that geometrical percolation depends on the geometrical shapes, e.g. randomly distributed spheres percolate at 0.3 while percolation of ellipsoids percolation depend on the aspect ratio of the ellipsoids.[16] Motivation of the percolation threshold for PEO is included in the main text.

AMORPHOUS STRUCTURES

The simulated PEO systems comprises 20 hydroxyl-terminated chains, each with 25 monomer units (1.11 kg/mol). This give a system size feasible for LS-DFT calculations and as shown below good prediction of the mass density. In addition, molecular weight has small impact of the refractive index[17] and it is expected that also electronic structure properties follow a similar trend. Indeed, electron localization seem to follow the Kuhn length of the polymer[18,19] which for PEO is ~8Å[20]. Different chain termination with elements already in the chain are not expected to impact the result either.

Initial configurations for neat and LiTFSI doped systems were generated using the PACKMOL package[21]. The salt concentrations considered in the salt doped systems were 12% wt, 25% wt and 50% wt. The initial configurations of the simulation boxes were generated through a random arrangement of polymer chains and ions, using the PACKMOL package[21]. General AMBER force field (GAFF) parameters[22] were used for describing bonding and non-bonding interactions in PEO and LiTFSI[23-25]. The AM1-BCC (bond charge correction)[26] model was used to assign the partial atomic charges.

GROMACS 2018.1[27,28] was used for MD simulations using leapfrog integrator with a time step of 1 fs. The long-range electrostatic interactions were employed through a particle mesh Ewald technique[29]. The short-range cutoff distances of the van der Waals and Coulomb interaction in the direct space are 1 nm. The bonds involving hydrogen atoms were constrained using the LINCS algorithm[30].

MD simulations in the NVT (constant number, volume, and temperature) ensemble was performed for the purpose of equilibration using a Bussi-Donadio-Parrinello thermostat[31] at 200, 300 and 400 K for 1 ns. Then NPT (constant number, pressure, and temperature) production runs using a Parrinello-Rahman barostat[32] and the same thermostat were performed at different temperatures for 10 ns simulation lengths, where the data were collected for analysis. During these simulations, the coupling constants for the thermostat and the barostat were set to 0.1 and 2.0 respectively.

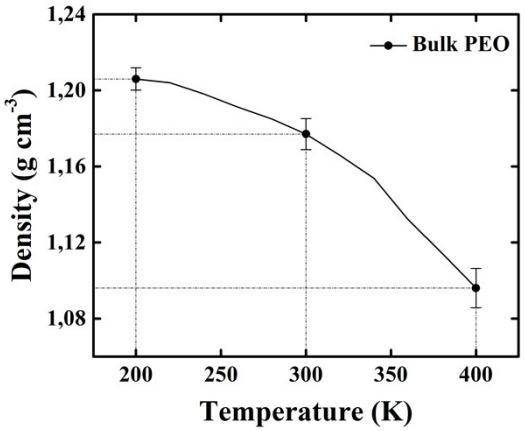

Figure S2 The average density of bulk PEO systems from MD simulations at different temperatures.

The density of the system was averaged over simulation time of 5 ns. The calculated average density at different temperatures were plotted in Figure S2. A few unique systems are then selected to be used in the LS-DFT calculations. For the neat PEO three different structures per temperature are included, these specific structures get densities 1.03-1.13 g/cm^3 depending on temperature. Single structures per LiTFSI concentration level are picked for the LiTFSI-PEO systems, which all are at 400 K.

REFERENCES

1. Skylaris, C.-K.; Haynes, P. D.; Mostofi, A. A.; Payne, M. C. Introducing ONETEP: Linear-scaling density functional simulations on parallel computers *J. Chem. Phys.* **2005**, *122*, 084119.
2. Perdew, J. P.; Burke, K.; Ernzerhof, M. Generalized Gradient Approximation Made Simple *Phys. Rev. Lett.* **1996**, *77*, 3865.
3. Elstner, M.; Hobza, P.; Frauenheim, T.; Suhai, S.; Kaxiras, E. Hydrogen bonding and stacking interactions of nucleic acid base pairs: A density-functional-theory based treatment *J. Chem. Phys.* **2001**, *114*, 5149.
4. Clark, S. J.; Segall, M. D.; Pickard, C. J.; Hasnip, P. J.; Probert, M. I. J.; Refson, K.; Payne, M. C. First principles methods using CASTEP *Zeitschrift für Kristallographie* **2005**, *220*, 567.

5. Adamo, C.; Barone, V. Toward reliable density functional methods without adjustable parameters: The PBE0 model *J. Chem. Phys.* **1999**, *110*, 6158.
6. Tkatchenko, A.; Scheffler, M. Accurate Molecular Van Der Waals Interactions from Ground-State Electron Density and Free-Atom Reference Data *Phys. Rev. Lett.* **2009**, *102*, 073005.
7. Ratcliff, L. E.; Hine, N. D. M.; Haynes, P. D. Calculating optical absorption spectra for large systems using linear-scaling density functional theory *Phys. Rev. B* **2011**, *84*, 165131.
8. Serra, S.; Tosatti, E.; Iarlori, S.; Scandolo, S.; Santoro, G. Interchain electron states in polyethylene *Phys. Rev. B* **2000**, *62*, 4389.
9. Moyassari, A.; Unge, M.; Hedenqvist, M. S.; Gedde, U. W.; Nilsson, F. First-principle simulations of electronic structure in semicrystalline polyethylene *J. Chem. Phys.* **2017**, *146*, 204901.
10. Takahashi, Y.; Tadokoro, H. Structural Studies of Polyethers, (-(CH2)m-O-)n. X. Crystal Structure of Poly(ethylene oxide) *Macromolecules* **1973**, *6*, 672.
11. Delley, B. From molecules to solids with the DMol3 approach *J. Chem. Phys.* **2000**, *113*, 7756.
12. Perdew, J. P.; Ruzsinszky, A.; Csonka, G. I.; Vydrov, O. A.; Scuseria, G. E.; Constantin, L. A.; Zhou, X.; Burke, K. Restoring the Density-Gradient Expansion for Exchange in Solids and Surfaces *Phys. Rev. Lett.* **2008**, *100*, 136406.
13. Delley, B. An all-electron numerical method for solving the local density functional for polyatomic molecules *J. Chem. Phys.* **1990**, *92*, 508.
14. Unge, M.; Christen, T. Electron and hole mobility edges in polyethylene from material simulations *Chem. Phys. Lett.* **2014**, *613*, 15.
15. Unge, M. Electron mobility edge in amorphous polyethylene *2016 IEEE International Conference on Dielectrics (ICD)* **2016**, *2*, 828.
16. Garboczi, E. J.; Snyder, K. A.; Douglas, J. F.; Thorpe, M. F. Geometrical percolation threshold of overlapping ellipsoids *Phys. Rev. E* **1995**, *52*, 819.
17. Ingham, J. D.; Lawson, D. D. Refractive index–molecular weight relationships for poly(ethylene oxide) *Journal of Polymer Science Part A: General Papers* **1965**, *3*, 2707.
18. Sato, M.; Kumada, A.; Hidaka, K. Multiscale modeling of charge transfer in polymers with flexible backbones *Phys. Chem. Chem. Phys.* **2019**, *21*, 1812.
19. Sato, M.; Kumada, A.; Hidaka, K. First-principles study of electron and hole transfer properties in various polymers *2018 IEEE 2nd International Conference on Dielectrics (ICD)* **2018**, 1.
20. García Sakai, V.; Maranas, J. K.; Chowdhuri, Z.; Peral, I.; Copley, J. R. D. Miscible blend dynamics and the length scale of local compositions *Journal of Polymer Science Part B: Polymer Physics* **2005**, *43*, 2914.
21. Martínez, L.; Andrade, R.; Birgin, E. G.; Martínez, J. M. PACKMOL: A package for building initial configurations for molecular dynamics simulations *Journal of Computational Chemistry* **2009**, *30*, 2157.
22. Wang, J.; Wolf, R. M.; Caldwell, J. W.; Kollman, P. A.; Case, D. A. Junmei Wang, Romain M. Wolf, James W. Caldwell, Peter A. Kollman, and David A. Case, 'Development and testing of a general amber force field'Journal of Computational Chemistry(2004) 25(9) 1157–1174 *Journal of Computational Chemistry* **2005**, *26*, 114.

23. Ebadi, M.; Costa, L. T.; Araujo, C. M.; Brandell, D. Modelling the Polymer Electrolyte/Li-Metal Interface by Molecular Dynamics simulations *Electrochim. Acta* **2017**, *234*, 43.
24. Sprenger, K. G.; Jaeger, V. W.; Pfaendtner, J. The General AMBER Force Field (GAFF) Can Accurately Predict Thermodynamic and Transport Properties of Many Ionic Liquids *J. Phys. Chem. B* **2015**, *119*, 5882.
25. Liu, H.; Paddison, S. J. Alkyl Chain Length Dependence of Backbone-to-Backbone Distance in Polymerized Ionic Liquids: An Atomistic Simulation Perspective on Scattering *Macromolecules* **2017**, *50*, 2889.
26. Jakalian, A.; Jack, D. B.; Bayly, C. I. Fast, efficient generation of high-quality atomic charges. AM1-BCC model: II. Parameterization and validation *Journal of Computational Chemistry* **2002**, *23*, 1623.
27. M.J. Abraham, D. v. d. S., E. Lindahl, B. Hess & and the GROMACS development team. GROMACS User Manual version 2018. (2018). Available at: www.gromacs.org. (Accessed: 19th June 2019).
28. Abraham, M. J.; Murtola, T.; Schulz, R.; Páll, S.; Smith, J. C.; Hess, B.; Lindahl, E. GROMACS: High performance molecular simulations through multi-level parallelism from laptops to supercomputers *SoftwareX* **2015**, *1-2*, 19.
29. Darden, T.; York, D.; Pedersen, L. Particle mesh Ewald: An N·log(N) method for Ewald sums in large systems *J. Chem. Phys.* **1993**, *98*, 10089.
30. Hess, B.; Bekker, H.; Berendsen, H. J. C.; Fraaije, J. G. E. M. LINCS: A linear constraint solver for molecular simulations *Journal of Computational Chemistry* **1997**, *18*, 1463.
31. Bussi, G.; Donadio, D.; Parrinello, M. Canonical sampling through velocity rescaling *J. Chem. Phys.* **2007**, *126*, 014101.
32. Parrinello, M.; Rahman, A. Polymorphic transitions in single crystals: A new molecular dynamics method *Journal of Applied Physics* **1981**, *52*, 7182.